Co-simulation Based Platform for Thermostatically Controlled Loads as a Frequency Reserve

*Aadil Latif, *Sohail Khan
Energy Department
Austrian Institute of Technology (AIT)
Vienna, Austria
{givenname.lastname}.fl@ait.ac.at

Peter Palensky
Electrical Engineering, Mathematics and Computer Science
TU Delft, Netherland

Wolfgang Gawlik
Institute of Energy Systems and Electrical Drives
TU Wien, Austria

***Abstract*—The rise in the intermittent power generation from renewables shall increase the secondary frequency reserve requirements in the future power system. Complimenting the support from the generators in providing frequency reserve, the active demand response can result in a cost effective contribution to this resource. Among demand response resources, the thermostatically controlled loads (TCLs) connected to the medium voltage networks poses an interesting potential. This work develops a co-simulation environment for the TCLs based demand side management scheme that can be used to assess the network impacts of using this service. An equivalent battery model with dynamic charging rate limits models the TCL aggregation and tracks a realistic frequency regulation signal. The co-simulation platform is tested for the IEEE 119 node distribution test feeder.**

***Index Terms*—smart grid, distributed control, communication, co-simulation**

NOMENCLATURE

i	Index of the TCL, from 1 to N.
k	Time index, from 1 to T.
θ^i	Temperature of i^{th} TCL.
Δ^i	Temperature dead-band width of i^{th} TCL.
ψ	Aggregate power deviation from the base value.
δ^i	Operational status of i^{th} TCL $\in (0,\ 1)$.
λ^i	TCL availability status $\in (0,\ 1)$.
π^i	Normalized temperature distance to the switching boundary of i^{th} TCL.
β^i	Control signal from central controller for i^{th} TCL $\in (-1,\ 0,\ 1)$.
ρ^i	Time duration after status change of i^{th} TCL.
$\overline{\rho^i}$	Short cycling duration of i^{th} TCL.
P^i, P_0^i	Rated and nominal power of i^{th} TCL.

I. INTRODUCTION

The primary goal in the power system operation is to balance supply and demand. Real time frequency regulation is paramount for the reliable operation of electricity network. Conventionally, generation units capable of quickly ramping up or down were installed with-in the network to cater for the deviations between supply and demand in the real time. The impact of the imbalance in active power results in frequency deviations. These deviation if gets large can violate the upper and lower limits of the frequency. This violation triggers the activation of frequency reserves in the system. For a European case, the decommissioning of the coal and nuclear power plants in the future shall decrease the capacity of the conventional generation in providing frequency reserves [1]. The anticipated rise in the share of generation from Renewable Energy Sources (RES) shall further increase the requirement of frequency reserves. Hence, the alternate sources of ancillary services are highly sought after.

Demand side management (DSM) means actively modifying the consumer's power demand pattern so that demand is regulated to follow generation. International Energy Agency (IEA) estimates that every \$ 1 investment in DSM is equivalent to \$ 2 investment in upgrading generation capabilities [2]. The Thermostatically Controlled Loads (TCLs) have an inherent flexibility in their operation. Appliances such as refrigerators, heaters, heat-pumps and air conditioners can be characterized as TCLs. All of such loads possess a common characteristic that the temperature is required to be maintained at a set-point. There is a dead-band around this point in which the TCL undergoes cycling process. The TCLs power consumption can be controlled with-in this dead-band without compromising on the comfort of the end customer. An aggregation of TCLs can be controlled similarly to track a reference power signal. The frequency regulation signal is essentially a power signal corresponding the mismatch of demand and supply. The TCL aggregation can be viewed as an energy storage that can participate in frequency regulation. The work in this paper is the extension of the battery model proposed in [3].

Two approaches are generally used for modeling the TCLs. Individual TCLs are most commonly modeled by a first order differential equation which captures the impact of the thermal properties of the loads, the state of the load and the ambient temperature. It calculates changes in temperature using the differential equation [4], [5]. The individual load model of the TCL as a combination of a continuous temperature

** These authors contributed equally to the work presented in the paper*

978-1-5090-1158-2/16/$31.00 ©2016 IEEE

state and a discrete "switching state" were first presented in [6]. The three state model capturing the temperature of thermal mass is discussed in [7]. More advanced models are discussed in the literature that aims to model the dynamics of TCL accurately [8]. The simulation of individual models can be challenging for large number of TCLs. However, this approach is suited for the simple control strategies [9]. The second approach is the state space modeling of the aggregation of TCLs. Among such methods, partial differential equation based approach is used for designing a sliding model control approach [10]. In [11] and [12], authors have proposed direct control over TCLs. In such a scenario, Distribution Network Operator (DNO) can change the state of the TCL via a direct control signal. The proposed scheme enables DNO to change the current power consumption of TCLs. In [13], authors have implemented control of TCLs using real time pricing data coordinated by the smart meters.

This work considers the individual TCL mode representing the thermal loads connected to a MV bus. A test-case based on co-simulation is developed in which the individual TCL model is implemented in PowerFactory and the central control is implemented in Python. The TCL aggregation tracks a reference frequency regulation signal and demonstrate the capabilities of both the tools.

The paper is organized as follows. Sec. II details the simulation setup covering tool selection, electrical network used and co-simulation setup. The model of TCL and stochastic battery is discussed in Sec. III. The implementation strategy of the stochastic limits based control is presented in Sec. III-C. In Sec. IV, the test case and results are discussed and followed by the conclusion in Sec. V.

II. Simulation setup

A. Tool selection

1) PowerFactory: PowerFactory is a domain specific tool for simulating, analyzing and understanding power systems [14]. The software package supports a power language called Digsilent Simulation Language (DSL) for implementing custom models and controllers while using RMS simulation. DSL however does not support matrices, which are required for the implementation of the central controller. For this work therefore, we have opted for a co-simulation approach where the power network and the local controllers for the TCLs have been implemented in PowerFactory and the central controller has been implemented in Python.

2) Python: Python is an open source high level scripting language with a large number of interdisciplinary tool boxes for optimization, signal processing, statistics, matrix calculations etc. This makes it an ideal option for implementing complex custom algorithms [15]. An added advantage of using Python is that being a high level language, comprehensive libraries are available for external coupling which require very little effort during implementation. Using co-simulation framework these toolboxes can be used in conjunction with PowerFactory to extend its capabilities.

B. Power Network

The network chosen for this work is an 11 kV radial MV test feeder comprising of 119 node. It consists of with 116 loads and 15 tie lines. The system data is given in Ref. [16]. In this work individual TCL power rating have been calculating using the Eqn. 1, where $U[0,1]$ is a uniform number between 0 and 1.

$$P_{TCL}^{i,rated} = 0.2 \times P_{load}^{i,rated} \times [U[0,1]+1] \ , \tag{1}$$

C. Co-simulation setup

PowerFactory supports a number of external interfaces covered in [17] in detail that can be used for data exchange with external software. In this work, PowerFactoy has been coupled with Python using sockets. DSL models are capable of making function calls to external C++ libraries. This ability has been used to implement socket communication support for local TCL controllers implemented within PowerFactory. Ease of implementation, re-usability and the ability to incorporate additional simulators for future work have been the main driving factors in selection of the simulation tools and the coupling scheme. An added advantage of the using the co-simulation approach is the ability to investigate the impact of DSM scheme on power network parameters such as voltage. Fig. 1 provides a graphical overview of the co-simulation setup.

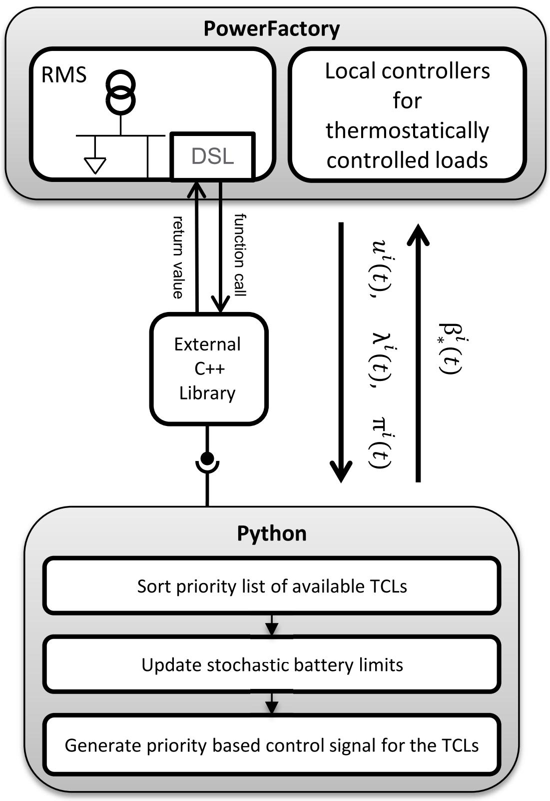

Fig. 1. Overview of the co-simulation setup

III. Control System Modeling

A. TCL modeling

In this work, TCLs have been modeled as first order difference equation (eq. 2). This TCL model is widely used for DSM studies in literature [6], [18], [19].

$$\theta^i[k+1] = g^i\theta^i[k] + (1-g^i)(\theta^i_a[k] - \delta^i[k]\theta^i_g) + \epsilon^i[k] \ , \quad (2)$$

where, $g^i = e^{-h/(R^iC^i)}$ (h is the sampling time and R^iC^i is the time constant of the TCL), $\theta^i_g = R^iP^i\eta^i$ and $\theta^i_a[k]$ is the ambient temperature measurement at the i^{th} TCL. The equation is weighted sum of the temperature at time k and the impact of the TCL on the temperature. The third term $\epsilon^i[k]$ is the noise associated with the temperature measurement at time k sampled from a normal distribution with mean 0 and standard deviation 0.5. P^i is the rated power of TCL which is positive in case of the air-conditioning load and negative for the heater. The state transition of the cooling TCL is given as [18],

$$\delta^i[k+1] = \begin{cases} 1 & \theta^i[k+1] > \theta^i_{\text{ref}} + \Delta^i \\ 0 & \theta^i[k+1] < \theta^i_{\text{ref}} - \Delta^i \\ \delta^i[k] & otherwise \end{cases} \ . \quad (3)$$

Each TCL implements a control algorithm 1. The input to this algorithm are the forced state changes from the central control $\beta^i[k]$. The TCL uses this information to update the variables of state (δ_i), availability (λ^i) and the relative temperature distance from the switching boundary (π^i).

A TCL is controllable only if its temperature θ^i is within the dead band Δ^i around the set reference temperature θ^i_{ref} and the cyclic time constraint is satisfied. If the temperature violates the dead band by more than 1.5 ^0C, local controller overrides the control signal from central control and turns the TCL ON/OFF depending on which temperature boundary has been violated.

Assuming during steady state operation, the temperature is equal to the reference temperature set by the consumer such that $\theta^i = \theta^i_{\text{ref}}$, power consumption can be calculated by solving the continuous power model from,

$$P^i_o[k] = \frac{\theta^i_a[k] - \theta^i_{ref}}{\eta^i R^i} \ . \quad (4)$$

During steady state operation, $P^i_o[k]$ is a valid estimation of average power consumed by the TCL in most cases [20]. Base power consumption is therefore sum of average power of all TCLs and is calculated using the equation,

$$P_{\text{base}}[k] = \sum_i P^i_o \ . \quad (5)$$

The instantaneous active power consumption at k^{th} time is the sum of the rated power of all active TCLs. It is given as,

$$P_{\text{agg}}[k] = \sum_i \delta^i[k]P^i \ . \quad (6)$$

The difference between the aggregate and base power consumption is termed as power deviation and is given as,

$$\psi[k] = P_{\text{agg}}[k] - P_{\text{base}}[k] \ . \quad (7)$$

In this work the TCL aggregation is modeled as a battery, which can charge or discharge depending on the reference power imbalance signal $r[k]$ and the power deviation $\psi[k]$. When $r[k] > \psi[k]$ battery is in charging state and TCLs are turning ON. Alternatively, when $r[t] < \psi[k]$ TCLs are being turned OFF and the battery is discharging. In order to use TCLs as a frequency reserve, the reference power imbalance signal, $r[k]$, must be followed in real-time.

Algorithm 1: Algorithm for local TCL controller

Input: Control signal - $\beta^i[k]$
Output: $(\delta_i[k+1],\ \lambda^i[k+1],\ \pi^i[k+1])$

$\theta^i[k+1] = g^i\theta^i[k] + (1-g^i)(\theta^i_a[k] - \delta^i[k]\theta^i_g) + \epsilon^i[k]$;
if $\rho^i[k] > \overline{\rho^i}$ **then**
  if $\underline{\theta^i} \leq \theta^i[k+1] \leq \overline{\theta^i}$ **then**
    $\lambda^i[k+1] = 1$;
    if $\beta^i[k] = 1$ **then**
      $\delta^i[k+1] = 1;\ \ \rho^i[k+1] = 0$;
    else if $\beta^i[k] = -1$ **then**
      $\delta^i[k+1] = 0;\ \ \rho^i[k+1] = 0$;
    else
      $\delta^i[k+1] = \delta^i[k]$
  else if $\theta^i[k+1] < \underline{\theta^i}$ **then**
    $\lambda^i[k+1] = 0;\ \ \delta^i[k+1] = 0;\ \ \rho^i[k+1] = 0$;
  else
    $\lambda^i[k+1] = 0;\ \ \delta^i[k+1] = 1;\ \ \rho^i[k+1] = 0$;
else
  $\lambda^i[k+1] = 0$;
  if $\theta^i[k+1] < \underline{\theta^i} - 1.5$ **then**
    $\delta^i[k+1] = 0;\ \ \rho^i[k+1] = 0$;
  else if $\theta^i[k+1] > \overline{\theta^i} + 1.5$ **then**
    $\delta^i[k+1] = 1;\ \ \rho^i[k+1] = 0$;
  else
    $\delta^i[k+1] = \delta^i[k]$
$\rho^i[k+1] = \rho^i[k] + 1$;
if $\delta^i[k+1] = 1$ **then** $\pi^i[k+1] \ = \ \left(\theta^i[k+1] - \underline{\theta^i}\right)/\Delta^i$;
if $\delta^i[k+1] = 0$ **then** $\pi^i[k+1] \ = \ \left(\underline{\theta^i} - \theta^i[k+1]\right)/\Delta^i$;

B. Stochastic Battery Model

The TCL aggregation can be modeled as a battery. The parameters of capacity C, ramp-up rate limit R_+ and ramp-down rate limits R_- are calculated as [20],

$$\begin{aligned} C &= \sum_i \left(1 + \left|1 - \frac{a_i}{\alpha}\right|\right)\frac{\Delta_i}{b_i} \\ R_+ &= \sum_i (P_i - P^o_i) \\ R_- &= \sum_i P^o_i \end{aligned} \quad , \quad (8)$$

here, $a_i = 1/(R_iC_i)$, $b_i = \eta_i/C_i$ and $d = 1/N\sum_i 1/(R_iC_i)$. This formulation enables the calculation of the maximum capacity [kWh] available in the battery model along with the ramp-rates. The consideration of the availability of TCLs enables the calculation of the stochastic parameters of the battery [3]. These parameters are given as,

$$\begin{aligned} C' &= \sum_i \lambda^i[k]\left(1+\left|1-\frac{a_i}{\alpha}\right|\right)\frac{\Delta_i}{b_i} \\ R'_+ &= R_+ - \sum_i (1-\lambda^i[k])P_i \\ R'_- &= R_- + \sum_i (1-\lambda^i[k])P_i \end{aligned} \quad , \tag{9}$$

where, the $\lambda^i[k]$ is the availability of i^{th} TCL given as ,

$$\lambda^i[k] = \begin{cases} 1 & \rho^i[k] > \bar{\rho^i} \ \&\ \underline{\theta}^i \le \theta^i[k] \le \bar{\theta}^i \\ 0 & \text{otherwise} \end{cases} \quad . \tag{10}$$

The stochastic ramp-limit constraint on the reference signal is considered by the following equation,

$$R'_- \le r[k] \le R'_+ \quad . \tag{11}$$

C. Supervisory Control

Each TCL communicates the variables of status, availability and temperature distance to the supervisory control. It is assumed that the control scheme has the record of the rated value of TCLs as part of the contract with the customers. In the first stage, the TCLs are categorized based on the operational state. For the On and available units a list is sorted based on the temperature distance (π). The TCLs having less distance to the switching boundary are given preference. This strategy reduces the switching frequency of TCLs. Same process is repeated for the Off and available units. The real time reference signal is filtered from the stochastic battery limits. The regulation signal is tracked by turning On/Off sufficient number of TCLs. The process is presented in Alg. 2. If a new TCL is added to the aggregation, its rated power is once communicated to the supervisory control, after which, it can participate in the frequency regulation process. The control signals generated by the central control β^i are communicated to the TCLs.

IV. Results and Discussion

A. Experiment Setup

The applicability of the proposed method is analyzed for 119-bus distribution system test case [21]. It is assumed that each bus has thermostatically controlled loads between 20% to 40% of the rated values. The upper limit of the flexible load is set to 50 kW for the experiment. Each bus may be representing a building with its thermal parameters modeled as equivalent thermal capacitance and resistance. The thermal capacitance per square meter varies between 0.015 to 0.065 kWh/°C. While thermal conductance varies between 0.001 to 0.003 kW/°C per square meter [22]. If a 14 kW of thermal load serves an area of 250 m^2, an approximate area of the building can be estimated using the rated thermal load value. The resulting thermal resistance can be calculated using $(R_{p.u.} \times \text{area})^{-1}$ and thermal capacitance by $C_{p.u.} \times \text{area}$. The parameters for each flexible load are sampled from the uniform

Algorithm 2: Algorithm at Main Control

Input : TCL i data $(u_i[k],\ \lambda^i[k],\ \pi^i[k])$
Output: Forced state of the TCL β^i_*

Calculate battery parameters $(C,\ n_+,\ n_-)$;
for $t := 1 \cdots T$ **do** *(Time iteration loop)*
    Sample input frequency regulation signal $r[k]$;
    for $i := 1 \cdots N$ **do** *(TCL iteration loop)*
        Sort priority list of available On/Off TCLs;
Update stochastic battery limits $(C',\ n'_+,\ n'_-)$;
if $(R'_+ \le r[k] \le R'_-)$ **then**
    $\xi = r[k] - \psi[k]$;
    if $r[k] < \psi[k]$ **then** *(Priority list based control)*
        Turn Off available TCLs till $\delta P < \xi$;
    else
        Turn On available TCLs till $\delta P < -\xi$;
else
    Regulation not possible;

distribution between the limits shown in Tab. I. The sampling time of 2 sec is used for the TCL model and for the reference signal tracking.

TABLE I
TCL PARAMETERS

Param.	Description	Value	Unit
θ_{ref}	Temperature set-point	$(21,\ 23)$	°C
Δ	Temperature dead-band	$(2,\ 3.2)$	°C
$\bar{\rho}$	Short cycling duration	$(16,\ 40)$	sec
η	Coefficient of performance	$(2.4,\ 2.6)$	

B. Results

Fig. 2 shows the temperature dynamics of a TCL around the reference value for a limited time interval of simulation. The control signal influence the operation while temperate remains within the dead-band.

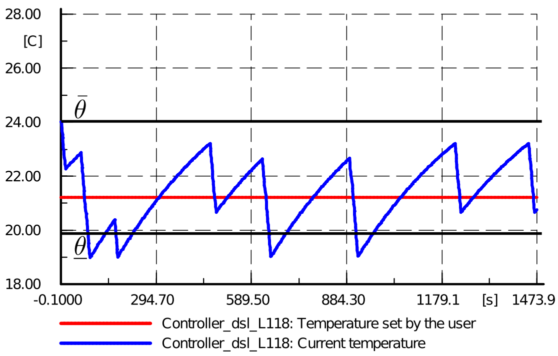

Fig. 2. TCL temperature dynamics

Fig. 3 shows how the temperature distance varies as function of the switching status. As the state changes the temperature distance is maximum from the switching boundary. It decreases with time unless the state change occurs.

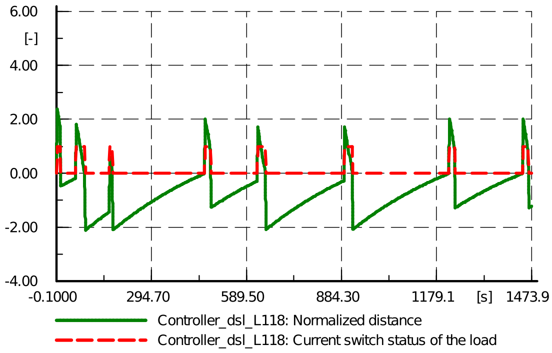

Fig. 3. TCL temperature distance from the switching boundary

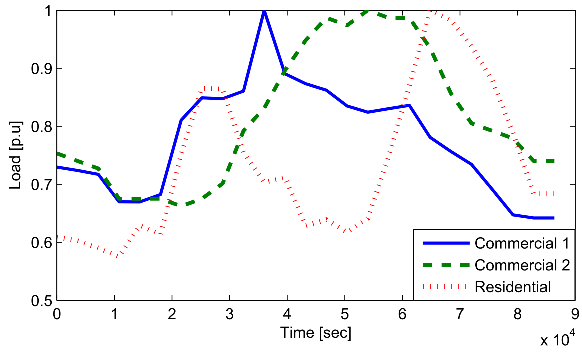

Fig. 5. Load profiles

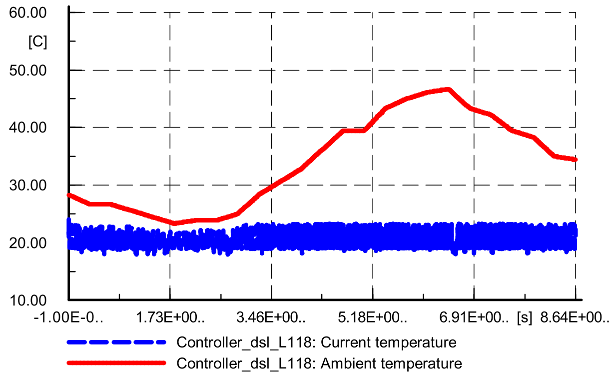

Fig. 6. TCL temperature dynamics

The tracking performance of proposed control scheme is shown in Fig. 4. It is observed that the TCL aggregation tend to follow the regulation signal dynamics. The precise regulation is not happening due to following reasons,

- Limited number of TCLs (116) are operating in the aggregation. Due to the high rating, each TCL is switched On/Off due to internal state transitions when temperature limits are violated.
- Some of the TCLs are not available as the cycling constraint has not been satisfied yet.

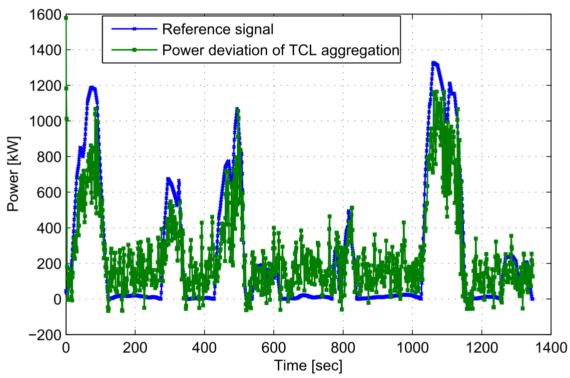

Fig. 4. Regulation signal tracking performance

In order to observe the impact of the frequency regulation on the network, a 24-hour simulation is implemented. This study aims to understand the impact of ambient temperature and the load forecast profiles on the frequency regulation. The loads are composed of the fixed and flexible thermal loads. Some of the loads are considered residential and others commercial. The profiles of both are shown in Fig. 5.

Fig. 6 shows the temperature in a TCL and the ambient temperature. It can be observed that despite the ambient temperature change the local TCL controller is able to keep the temperature with-in the limits along with serving for the frequency regulation. The availability of the TCLs has a strong correlation with the difference between the ambient and the internal temperature as shown in Fig. 7. When the temperature is high, the frequency of air conditioning loads being turned On/Off increase. Due to the cycling constraint, the number of available TCLs decreases.

The impact of the frequency regulation and the ambient temperature at the end of a feeder (bus 80) can be seen in Fig. 8. The simulation platform enables to design the control schemes that can take the voltage limits at the end of the feeder as constraints.

C. Outlook

The presented simulation platform is useful to study the impact of frequency regulation on the distribution network. It shall be important to ensure that any control scheme implemented does not result in the constraint violations. The co-simulation platform enables to use the features of Power Factory in the control scheme, thus opening new areas of research and possibilities. The consideration of the communication delays, accuracy of the communicated data and uncertainty in measurement at the local control shall further influence the

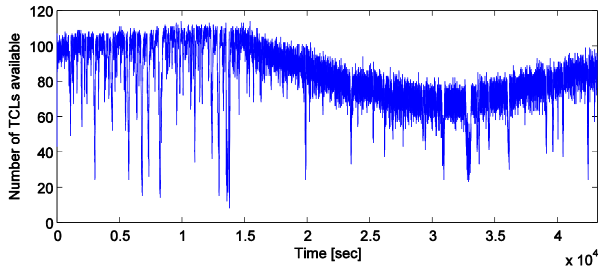

Fig. 7. TCL availability

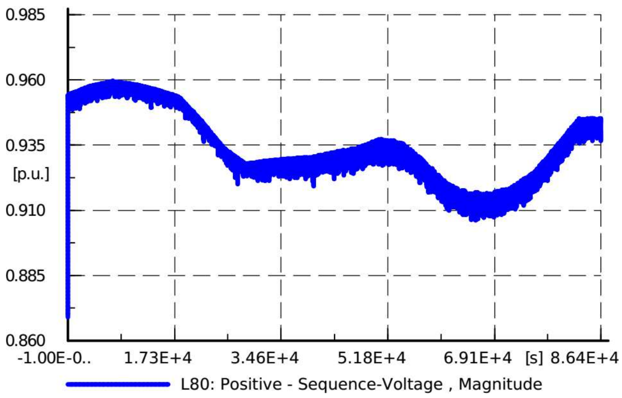

Fig. 8. Bus voltage dynamics

tracking performance.

V. Conclusion

This paper builds upon the existing literature for modeling TCL aggregation.The 119 node distribution network and local thermostatic controllers for the loads have been modeled in PowerFactory. Aggregated TCLs have been modeled using a battery which has been implemented in Python. Battery's dynamic parameters such as state of charge and charging limits have been modeled a function of available resources. Communication between the two simulation tools has been achieved via socket. The Results show that TCL based DSM schemes can be used as frequency reserve.

References

[1] ENTSO-E. (2015) Entso-e scenario outlook & adequacy forecast (so&af) 2015. Accessed: 2016-01-10. [Online]. Available: https://www.entsoe.eu/publications/system-development-reports/adequacy-forecasts/Pages/default.aspx

[2] S. O. service), *World energy outlook*. OECD/IEA, 2006.

[3] S. Khan, M. Shahzad, U. Habib, W. Gawlik, and P. Palensky, "Stochastic Battery Model for Aggregation of Thermostatically Controlled Loads," *ArXiv e-prints*, Jan. 2016.

[4] M. Liu, Y. Shi, and X. Liu, "Distributed mpc of aggregated heterogeneous thermostatically controlled loads in smart grid," 2016.

[5] S. Esmaeil Zadeh Soudjani and A. Abate, "Aggregation and control of populations of thermostatically controlled loads by formal abstractions," *Control Systems Technology, IEEE Transactions on*, vol. 23, no. 3, pp. 975–990, 2015.

[6] S. Ihara and F. Schweppe, "Physically based modeling of cold load pickup," *Power Apparatus and Systems, IEEE Transactions on*, vol. PAS-100, no. 9, pp. 4142–4150, Sept 1981.

[7] W. Zhang, J. Lian, C.-Y. Chang, and K. Kalsi, "Aggregated modeling and control of air conditioning loads for demand response," *Power Systems, IEEE Transactions on*, vol. 28, no. 4, pp. 4655–4664, Nov 2013.

[8] K. Schneider, J. Fuller, and D. Chassin, "Multi-state load models for distribution system analysis," *Power Systems, IEEE Transactions on*, vol. 26, no. 4, pp. 2425–2433, Nov 2011.

[9] S. Koch, M. Zima, and G. Andersson, "Active coordination of thermal household appliances for load management purposes," in *IFAC Symposium on Power Plants and Power Systems Control*. Citeseer, 2009.

[10] S. Bashash and H. Fathy, "Modeling and control of aggregate air conditioning loads for robust renewable power management," *Control Systems Technology, IEEE Transactions on*, vol. 21, no. 4, pp. 1318–1327, July 2013.

[11] S. Kundu, N. Sinitsyn, S. Backhaus, and I. Hiskens, "Modeling and control of thermostatically controlled loads," *arXiv preprint arXiv:1101.2157*, 2011.

[12] S. E. Z. Soudjani and A. Abate, "Aggregation of thermostatically controlled loads by formal abstractions," in *European Control Conference, Zurich, Switzerland*, 2013.

[13] S. Li, W. Zhang, J. Lian, and K. Kalsi, "Market-based coordination of thermostatically controlled loads –part i: A mechanism design formulation," *Power Systems, IEEE Transactions on*, vol. PP, no. 99, pp. 1–9, 2015.

[14] D. Powerfactory, "Powerfactory users manual," *DIgSILENT, GmbH*, vol. 14, 2011.

[15] G. VanRossum and F. L. Drake, *The Python Language Reference*. Python software foundation Amsterdam, Netherlands, 2010.

[16] S. Ghasemi and J. Moshtagh, "Radial distribution systems reconfiguration considering power losses cost and damage cost due to power supply interruption of consumers," *International Journal on Electrical Engineering and Informatics*, vol. 5, no. 3, p. 297, 2013.

[17] A. Latif, M. Shahzad, P. Palensky, and W. Gawlik, "An alternate powerfactory matlab coupling approach," in *Smart Electric Distribution Systems and Technologies (EDST), 2015 International Symposium on*. IEEE, 2015, pp. 486–491.

[18] J. Mathieu, M. Kamgarpour, J. Lygeros, and D. Callaway, "Energy arbitrage with thermostatically controlled loads," in *Control Conference (ECC), 2013 European*, July 2013, pp. 2519–2526.

[19] R. Mortensen and K. Haggerty, "Dynamics of heating and cooling loads: models, simulation, and actual utility data," *Power Systems, IEEE Transactions on*, vol. 5, no. 1, pp. 243–249, Feb 1990.

[20] H. Hao, B. Sanandaji, K. Poolla, and T. Vincent, "Aggregate flexibility of thermostatically controlled loads," *Power Systems, IEEE Transactions on*, vol. 30, no. 1, pp. 189–198, Jan 2015.

[21] R. Srinivasa Rao, S. Narasimham, M. Ramalinga Raju, and A. Srinivasa Rao, "Optimal network reconfiguration of large-scale distribution system using harmony search algorithm," *Power Systems, IEEE Transactions on*, vol. 26, no. 3, pp. 1080–1088, Aug 2011.

[22] D. S. Callaway, "Tapping the energy storage potential in electric loads to deliver load following and regulation, with application to wind energy," *Energy Conversion and Management*, vol. 50, no. 5, pp. 1389 – 1400, 2009.